

Supporting Information for the article “New Strontium-based Bioactive Glasses: Physicochemical Reactivity and Delivering Capability of Biologically Active Dissolution Products”

Jonathan Lao, Jean-Marie Nedelec, and Edouard Jallot.

1 Chemical composition of the sol-gel derived SiO₂-CaO-SrO and SiO₂-CaO-P₂O₅-SrO glasses

The experimental compositions are close to the expected nominal values (Table 1). One can note that the total amount in oxide sums up to about 97-98 %; indeed the glasses are highly reactive towards water due to their high alkaline-earth content. Thus they can easily become hydrated in contact with the air and ambient carbon dioxide can penetrate into the highly porous samples, condensing at the materials surface to form calcium carbonate

	B75	B75-Sr1	B75-Sr5	B67.5	B67.5-Sr1	B67.5-Sr5
SiO ₂	72.20 ± 0.37	74.22 ± 0.52	74.08 ± 0.51	63.75 ± 0.40	67.16 ± 0.47	64.93 ± 0.45
P ₂ O ₅	–	–	–	6.95 ± 0.14	7.04 ± 0.14	7.62 ± 0.15
CaO	24.50 ± 0.17	23.60 ± 0.17	19.03 ± 0.13	24.13 ± 0.11	23.31 ± 0.16	20.25 ± 0.14
SrO	72.20 ± 0.37	0.83 ± 0.08	3.83 ± 0.04	63.75 ± 0.40	0.81 ± 0.08	4.27 ± 0.04

Table 1. Composition of (weight %) as determined by ICP-AES

2 N₂ sorption analyses of the glass powders

The BET surface area, the average and modal pore diameters and the total pore volume have been calculated (see Table 2). The surface area and the total pore volume increase with the phosphorus content. For all the glasses, large pore size distributions were observed: the pores ranged from 3 nm to 80 nm in diameter. However, both the modal and average pore diameters increase with the phosphorus content. These results have already been discussed in a previous work (see Ref.12 in the article). Regarding the addition of strontium in the glassy matrix, it leads to a decrease in the specific surface area and an increase in the average pore diameter. Although Sr assumes the same role of

network modifier as Ca, it owns distinct physicochemical properties that lead to specific texture and porosity properties for strontium-doped materials.

	B75	B75-Sr1	B75-Sr5	B67.5	B67.5-Sr1	B67.5-Sr5
BET surface area (m ² /g)	30	24	28	112	99	39
BJH average pore diameter (nm)	8.4	11.8	9.3	13.2	11.7	28.2
BJH modal pore diameter (nm)	4.6	6.1	4.7	8.9	6.2	4.6
Total pore volume (cm ³ /g)	0.062	0.069	0.066	0.289	0.222	0.245

Table 1. N₂ sorption analyses of the gel-glass powders. The surface area (S) was determined from the linear portion of the BET plot, the total pore volume (V) was estimated from the amount of N₂ adsorbed at P/P₀ = 0.995, the pore size distribution and the modal pore diameter were calculated by applying the BJH method to the N₂ desorption branches, and the average pore diameter was calculated as $r = 2V/S$.

3 Chemical mapping of the glass disc/biological fluids interface

Here are some supplementary figures concerning the distribution of elements at the interface between the SiO₂–CaO–SrO and SiO₂–CaO–P₂O₅–SrO glass discs and biological fluids after 6 hours of interaction.

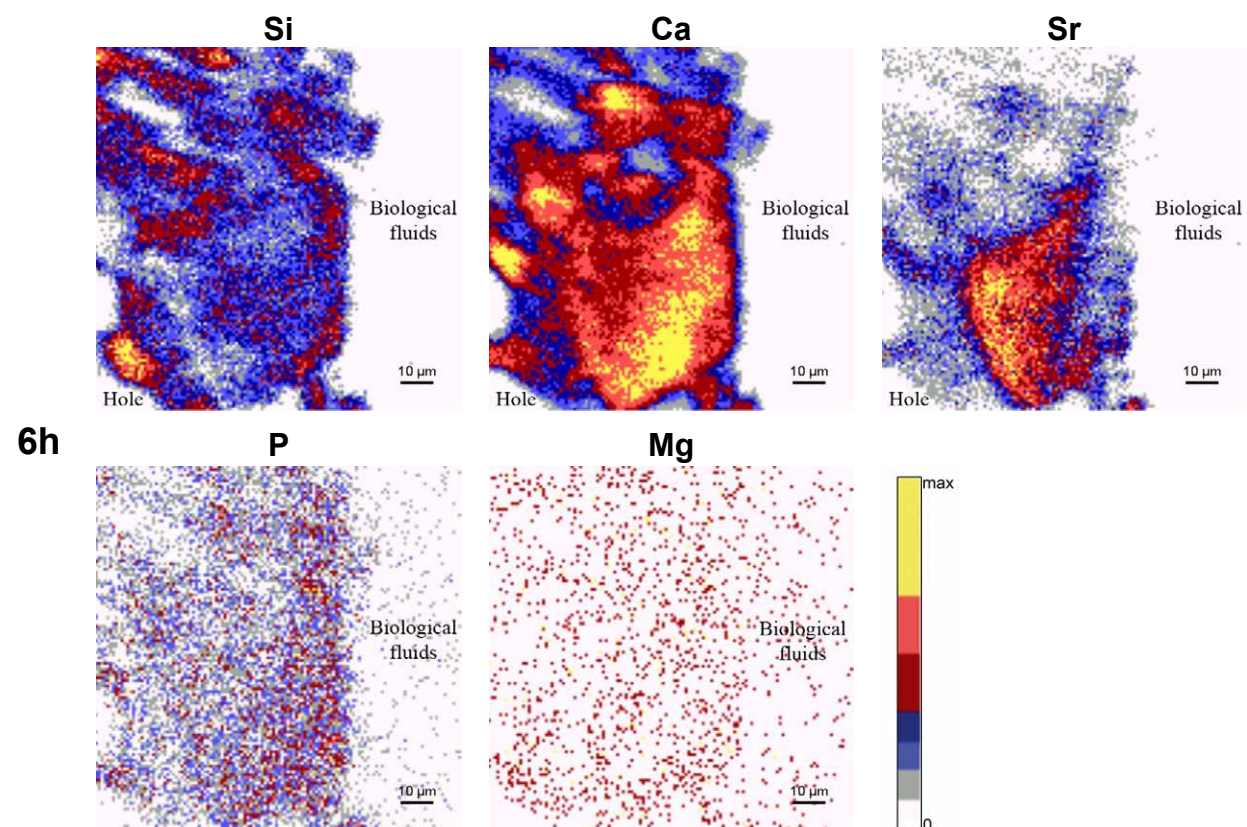


Figure 1. Elemental maps at the periphery of a SiO₂–CaO–SrO B75–Sr5 glass disc after 6 hours of interaction with biological fluids

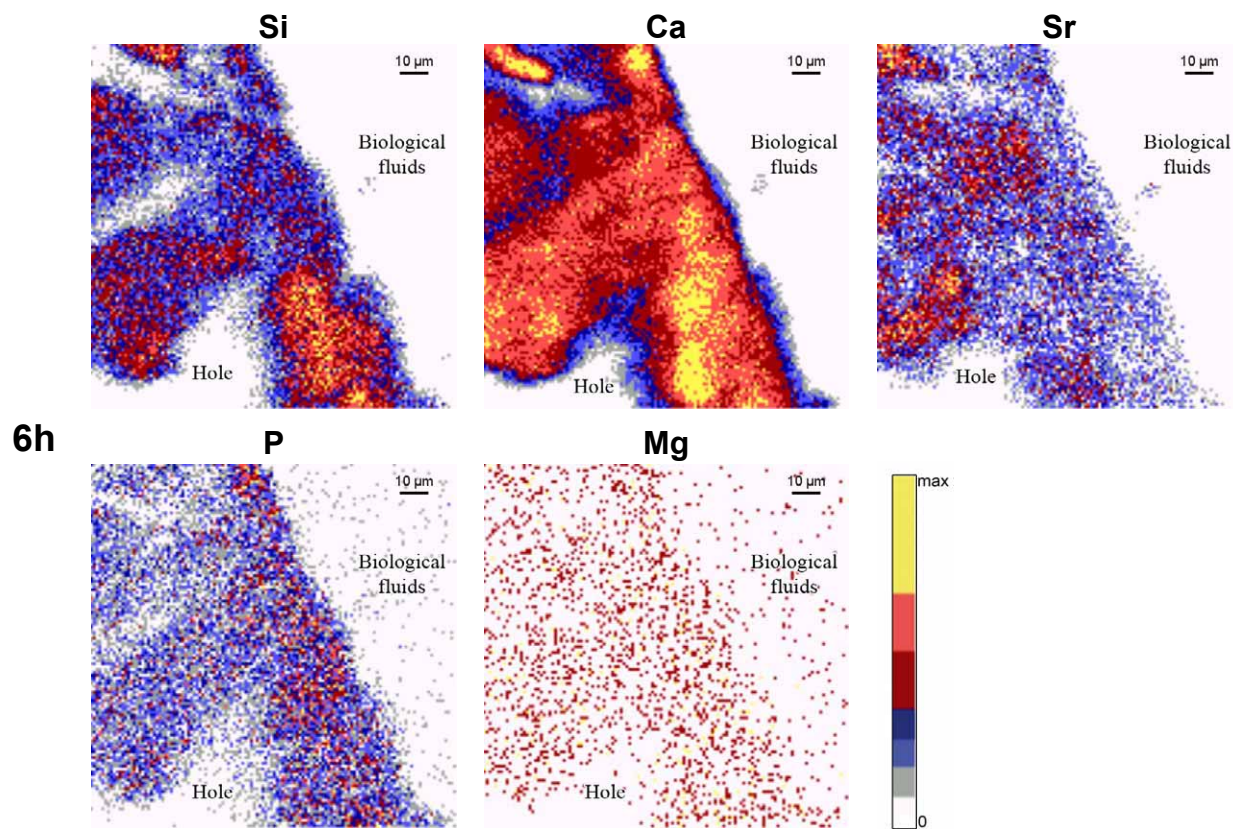


Figure 2. Elemental maps at the periphery of a $\text{SiO}_2\text{--CaO--P}_2\text{O}_5\text{--SrO}$ B67.5-Sr5 glass disc after 6 hours of interaction with biological fluids

4 Evolution of elemental concentrations at the periphery and in the inner regions of the glass discs

See the Article for a complete description of the figures.

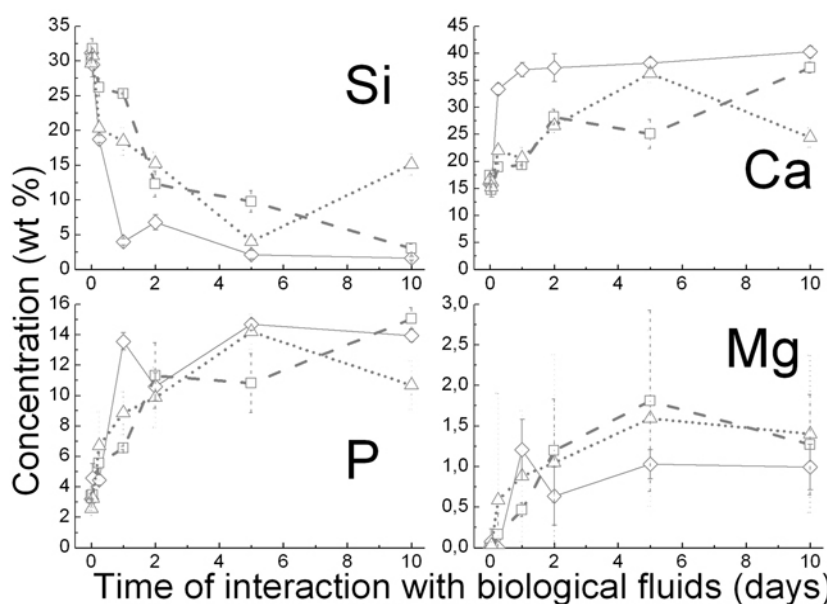


Figure 3. Evolution of elemental concentrations at the periphery of the $\text{SiO}_2\text{--CaO--P}_2\text{O}_5\text{--SrO}$ glass discs with time of exposure to biological fluids, $-\diamond-$ B67.5, $--\square--$ B67.5-Sr1, $\cdot\cdot\triangle\cdot\cdot$ B67.5-Sr5.

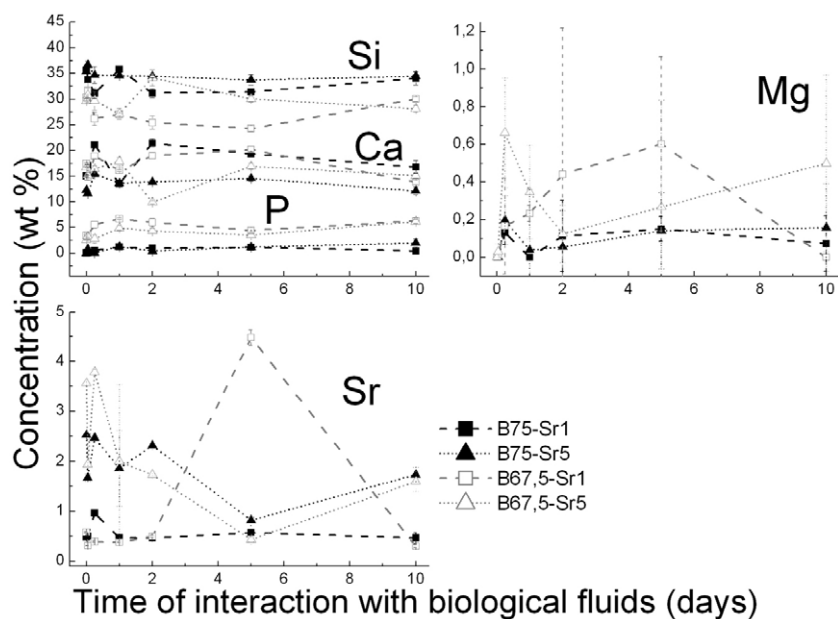


Figure 4. Evolution of elemental concentrations in the inner regions of the $\text{SiO}_2\text{--CaO}\text{--SrO}$ and $\text{SiO}_2\text{--CaO}\text{--P}_2\text{O}_5\text{--SrO}$ glass discs with time of exposure to biological fluids.

5 Evolution of elemental concentrations at the periphery of the glass particles

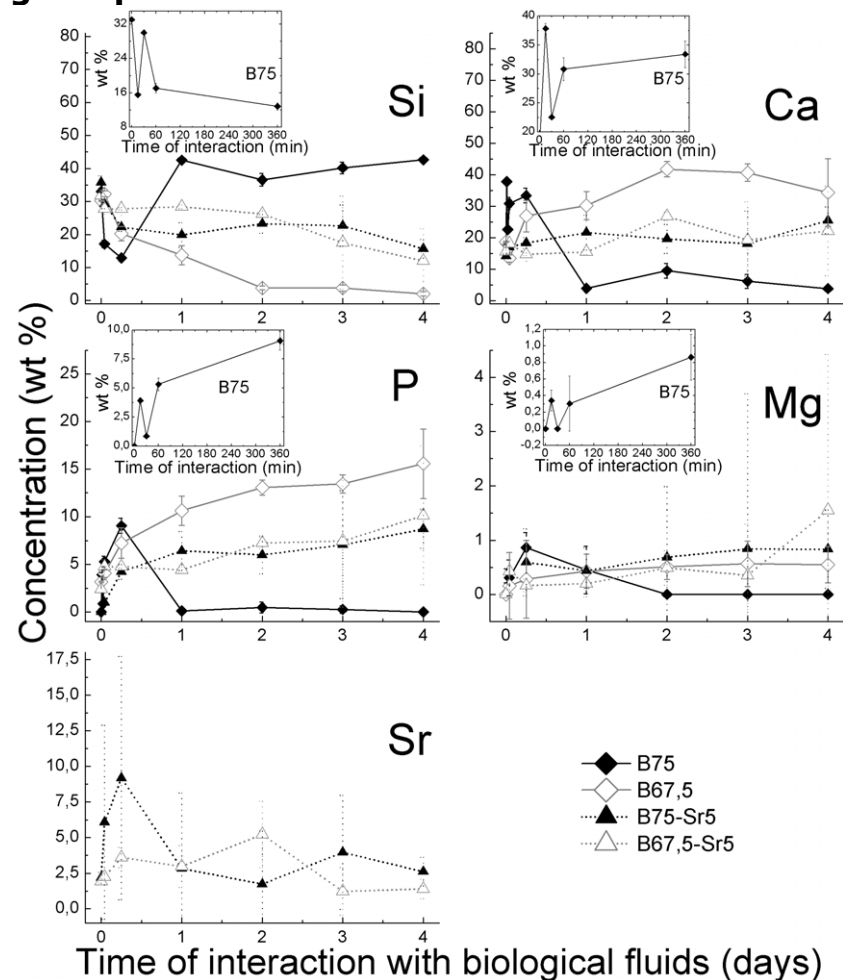


Figure 5. Evolution of elemental concentrations at the periphery of the glass particles with time of exposure to biological fluids.

6 Composition of biological fluids during interaction with the glass particles

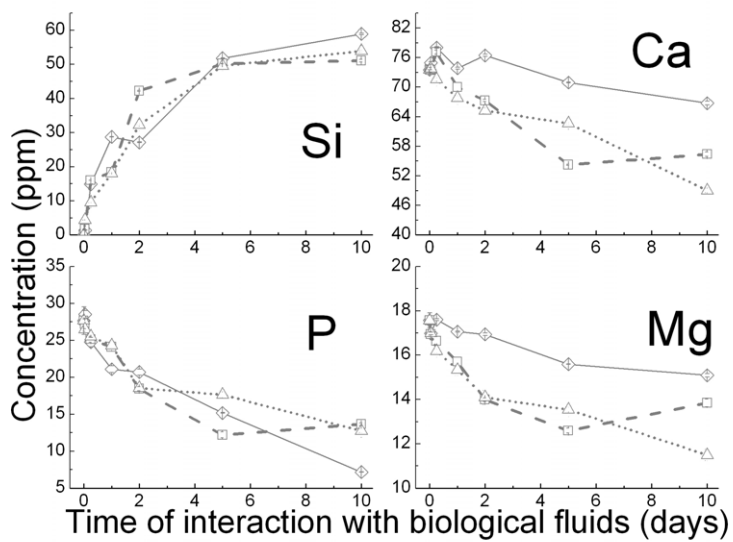


Figure 6: Evolution of elemental concentrations in biological fluids with time of interaction with $\text{SiO}_2\text{--CaO--P}_2\text{O}_5\text{--SrO}$ glass discs, \diamond B67.5, \square B67.5-Sr1, \triangle B67.5-Sr5.

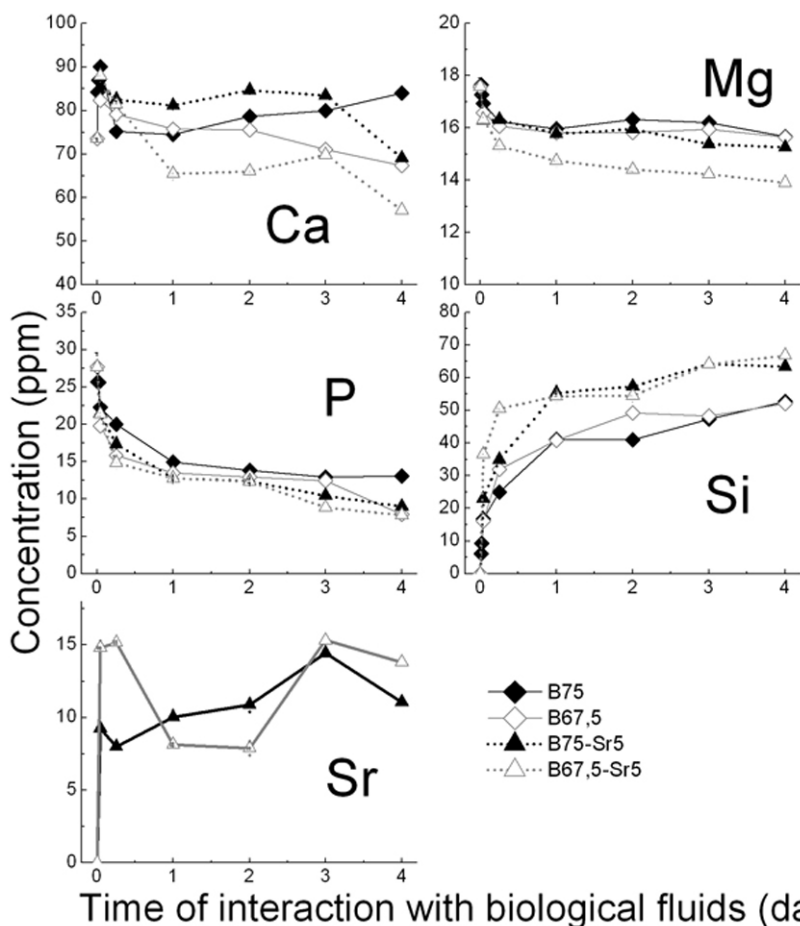


Figure 7. Evolution of elemental concentrations in biological fluids with time of interaction with the glass particles.